Inorganic Chemistry

Article

pubs.acs.org/IC

Putting a Terbium-Monometallic Cyanide Cluster into the C_{82} Fullerene Cage: TbCN@C_2(5)-C_{82}

Fupin Liu, Song Wang, Jian Guan, Tao Wei, Minxiang Zeng, and Shangfeng Yang*

Hefei National Laboratory for Physical Sciences at Microscale, CAS Key Laboratory of Materials for Energy Conversion & Department of Materials Science and Engineering, Synergetic Innovation Center of Quantum Information & Quantum Physics, University of Science and Technology of China (USTC), Hefei 230026, People's Republic of China

Supporting Information

ABSTRACT: The first terbium (Tb)-monometallic cyanide clusterfullerene (CYCF), TbCN@C_{82}, has been successfully synthesized and isolated, whose molecular structure was determined unambiguously as TbCN@C_2(5)-C_{82} by single crystal X-ray diffraction. The C_2(5)-C_{82} isomeric cage represents a new cage capable of encapsulating a monometallic cyanide cluster. The C−N bond length within the encaged TbCN cluster is determined to be 0.94(5) Å, which is smaller by at least 0.17 Å than those of the reported C−N triplet bonds in traditional cyanide/nitrile compounds and cyano coordination complexes. An electronic configuration of $[Tb^{3+}(CN)^-]^{2+}@[C_{82}]^{2-}$ was proposed for TbCN@C_{82}.

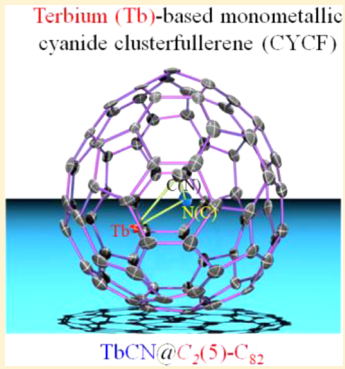

INTRODUCTION

As a special family of carbon nanostructures, endohedral fullerenes with atoms, ions, or clusters encapsulated in the interior of carbon cages have shown unique molecular structures and electronic, physical/chemical properties as well as potential applications in biomedicine and organic photovoltaics, and so forth.[1] Among them, clusterfullerenes are characteristic in the encapsulation of an unstable metallic cluster by a robust fullerene cage which is in some cases unstable as well.[1f] As the first metal nitride clusterfullerene (NCF),[2] $Sc_3N@C_{80}$ was synthesized in 1999 by a modified Krätschmer−Huffman DC-arc discharging method with the addition of N_2.[2a] Because of the considerably high yield, the discovery of $Sc_3N@C_{80}$ initiated a new era of endohedral fullerene research, and led to the consequent discovery of five other types of clusterfullerenes,[1f] including carbide clusterfullerenes (CCFs),[3] oxide clusterfullerenes (OCFs),[4] sulfide clusterfullerenes (SCFs),[5] hydrocarbide clusterfullerenes (HCCFs),[6] and carbonitride clusterfullerenes (CNCFs).[7] Specifically, as the well-established method to synthesize NCFs, the addition of N_2 in the Krätschmer−Huffman DC-arc discharging process appears particularly important because not only clusterfullerenes including NCFs and CNCFs but also endohedral azofullerenes in the form of $M_2@C_{79}N$ (M = Y, Tb, Gd) can be synthesized simultaneously.[2,7,8] Furthermore, using the same modified Krätschmer−Huffman DC-arc discharging method with the addition of N_2 while TiO_2 was added in the raw mixture, very recently we discovered the first monometallic cyanide clusterfullerene (CYCF), YCN@C_s(6)-C_{82}, for which the formation was fullfilled only with the introduction of TiO_2 in the raw mixture.[9] The discovery of such a monometallic clusterfullerene is significant because in previous reports it was revealed that monometallofullerenes always existed as a simple form of M@C_{2n} and clusterfullerenes always required multiple (two to four) metal cations to stabilize an unstable metal cluster.[1,9] Given that so far YCN@C_s(6)-C_{82} is the only reported CYCF, an intriguing question to be addressed is whether other rare earth metals and cage isomers could form the CYCF structure or not. Herein, we report the synthesis, isolation, and structural characterization of the first terbium (Tb)-based CYCF, TbCN@C_2(5)-C_{82}. The molecular structure of TbCN@C_2(5)-C_{82} was determined unambiguously by single crystal X-ray diffraction, and its electronic property was characterized by UV−vis−NIR spectroscopy and electrochemistry.

RESULTS AND DISCUSSION

Synthesis and Isolation of TbCN@C_{82}. TbCN@C_{82} was synthesized by a modified Krätschmer−Huffman DC-arc discharge method using a mixture of Tb_4O_7 and graphite (molar ratio of Tb/C = 1:15) as the raw material under 400 mbar He and 10 mbar N_2 gas.[10,11] Since the addition of TiO_2 in the raw mixture was found to be essential for the synthesis of the reported YCN@C_{82},[9] in our present study, we also investigated the effect of TiO_2 on the formation of TbCN@C_{82} by blending TiO_2 with the mixture of Tb_4O_7 and graphite (molar ratio of Tb/Ti/C = 1:1:15), which was subject to arc discharge under the identical conditions. Interestingly, TbCN@C_{82} was observed in both fractions **A** and **A′** obtained from the

Received: February 12, 2014
Published: May 1, 2014

   dx.doi.org/10.1021/ic500353k | Inorg. Chem. 2014, 53, 5201−5205

extracts of Tb_4O_7/N_2 and $Tb_4O_7/TiO_2/N_2$, respectively, revealing that TiO_2 is not essential to the formation of $TbCN@C_{82}$ (see Supporting Information, SI, Figures S1 and S2). This result is contrary to the case of $YCN@C_{82}$ for which the addition of TiO_2 in the raw mixture was essential,[9] suggesting that the formation of CYCF is sensitively dependent on the nature of the encapsulated rare earth metal.

Isolation of $TbCN@C_{82}$ was accomplished by three-step HPLC (see SI S1 for details), and the high purity of the isolated $TbCN@C_{82}$ sample was confirmed by laser desorption/ionization time-of-flight (LD-TOF) mass spectroscopy (MS), indicating a predominant mass peak at m/z = 1169. Besides, the isotopic distribution analysis of the measured mass peak at m/z = 1169 shows a good coincidence with the calculated one (see SI Figure S4), confirming the proposed chemical identification of $TbC_{83}N$.

X-ray Crystallographic Study of $TbCN@C_2(5)$-C_{82}. The molecular structure of $TbCN@C_{82}$ was determined unambiguously to be $TbCN@C_2(5)$-C_{82} by X-ray crystallographic study performed on a cocrystal of $TbCN@C_{82}$ with $Ni^{II}(OEP)$ (OEP = octaethylporphyrin), which was obtained by layering a benzene solution of $TbCN@C_{82}$ over a benzene solution of $Ni^{II}(OEP)$.[12] Figure 1 shows the relative orientations of the

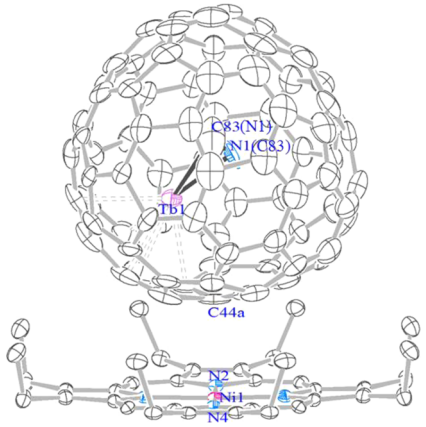

Figure 1. Drawing showing the interaction between the fullerene and porphyrin in $TbCN@C_2(5)$-C_{82}·$Ni^{II}(OEP)$·$2C_6H_6$ with 25% thermal ellipsoids. C, N, Tb, and Ni atoms are shown in gray, slate blue, orchid and deep pink, respectively. Only one orientation of the fullerene cage (0.50 occupancy) and the most abundant Tb site with 0.217 fractional occupancy are shown. The solvent molecule (benzene), another orientation of the fullerene cage, the minor metal positions, and hydrogen atoms of the porphyrin are all omitted for clarity.

$TbCN@C_2(5)$-C_{82} and the $Ni^{II}(OEP)$ molecules in $TbCN@C_2(5)$-C_{82}·$Ni^{II}(OEP)$·$2C_6H_6$ cocrystal. Only one orientation of the fullerene cage together with the major site of TbCN cluster was shown in the drawing for clarity. This structure reveals clearly that the carbon cage is composed of 82 atoms with $C_2(5)$ symmetry, thus ruling out the possibility of the endohedral azafullerene structure $Tb@C_{83}N$ with an 84-atom carbon cage.

The asymmetric unit cell of the cocrystal $TbCN@C_2(5)$-C_{82}·$Ni^{II}(OEP)$·$2C_6H_6$ contains a half of the $Ni^{II}(OEP)$ molecule and two halves of the $C_2(5)$-C_{82} cage. The crystallographic mirror bisects N2, N4, Ni1, and C83(N1) and is perpendicular to the paper plane as shown in Figure 1. The fully ordered $Ni^{II}(OEP)$ is present on the crystallographic mirror that bisects N2, N4, and Ni1, so an intact $Ni^{II}(OEP)$ molecule was readily obtained by combining the existing half molecule with its mirror image. The nearest cage-Ni contact involves C44a with a distance of 2.82(2) Å, which is similar to those reported for cocrystals of other endohedral fullerenes with $Ni^{II}(OEP)$.[12d,13] A complete C_{82} cage was finally obtained by combining one of the halves of the fullerene cage with the mirror image of the other. Accordingly, the occupancies of the two cage orientations are 0.50, respectively.

Similar to the cases of other clusterfullerenes, the encaged TbCN cluster shows disorder.[4,14] As shown in Figure 2, for the

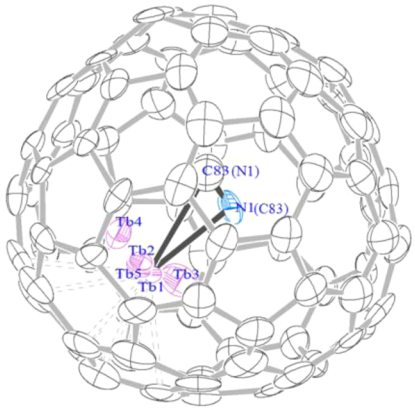

Figure 2. Drawing showing one orientation of the fullerene cage together with a half of the Tb disordered sites with 25% thermal ellipsoids, another half of the Tb disordered sites could be generated by mirror plane of the crystal. The fractional occupancies are 0.217, 0.138, 0.067, 0.056, and 0.022 for Tb1, Tb2, Tb3, Tb4, and Tb5, respectively.

encapsulated TbCN cluster, as many as ten sites for Tb are distinguishable (with occupancies 0.217, 0.138, 0.067, 0.056, and 0.022 for Tb1, Tb2, Tb3, Tb4, and Tb5, respectively, another five sites are generated by the mirror image of these five Tb sites (see SI Figure S6)). However, two sites for the CN moiety were distinguishable, but differentiation between carbon and nitrogen atoms is challenging because of their similarity on the size and scattering power.[8a] Despite such an ambiguity, clearly one atom (C83 or N1) locates on the crystallographic mirror plane, while another site (N1 or C83) is generated by the crystallographic mirror which is vertically perpendicular to the paper plane as shown in Figure 2.

Similar to the structure of the recently isolated $YCN@C_s(6)$-C_{82},[9] both C and N atoms within the encapsulated TbCN cluster are located near the cage center, whereas Tb atom locates between the CN unit and one side of the cage, affording a triangular TbCN cluster which is different from the linear structures commonly found in traditional metal cyanide complexes (see also SI Figure S5).[15] For the major Tb site with a 0.217 occupancy (Tb1), the Tb1−N1 (C83), and Tb1−C83 (N1) bond distances are 2.32(3) Å and 2.36(5) Å, respectively, and this shows a similar trend with that of $YCN@C_s(6)$-C_{82}, in which the bond distances of Y−N and Y−C (the major Y site) are 2.383 and 2.484 Å, respectively.[9] Even more intriguingly, the C−N bond length within $TbCN@C_2(5)$-C_{82} is determined to be 0.94(5) Å, which is very close to that within $YCN@C_s(6)$-C_{82} (0.935 Å).[9] Such a short C−N bond is quite unusual, because it is shorter by at least 0.17 Å than those of the reported C−N triple bonds in traditional cyanide/nitrile compounds and cyano coordination complexes (1.12−1.17

dx.doi.org/10.1021/ic500353k | Inorg. Chem. 2014, 53, 5201−5205

Å).[9,15] Similar to the case of YCN@C_s(6)-C_{82}, this finding on the unusually short C−N bond within TbCN@C_2(5)-C_{82} reveals once more the unique bonding feature of the TbCN cluster upon encapsulated in carbon cage, and such a shrinking effect may be interpreted by the stronger bonding between metal and C/N atoms induced by the space confinement of the interior of the carbon cage.[9] Besides, because the C−N bond length of TbCN@C_2(5)-C_{82} is also much smaller than the C−C bond lengths of all carbide clusterfullerenes determined by X-ray crystallographic study as well, for which the smallest C−C bond length was reported to be 1.04 Å for Gd_2C_2@D_3(85)-C_{92},[16] a possible carbide clusterfullerene TbC_2@$C_{81}N$ as an isomeric structure of TbCN@C_{82} can be excluded.

Electronic Absorption and Vibrational Spectroscopic Study of TbCN@C_2(5)-C_{82}. Figure 3 presents the UV−vis−NIR absorption spectrum of the isolated TbCN@C_2(5)-C_{82} dissolved in toluene (curve a) in comparison with that of the reported YCN@C_s(6)-C_{82} (curve b). The electronic absorption spectrum of TbCN@C_2(5)-C_{82} exhibits one broad shoulder peak at about 392 nm along with a broad absorption peak with three absorption maxima at 627, 656, and 763 nm in the UV and visible regions and a distinct absorption peak at 1056 nm accompanied by a weak absorption peak at 923 nm in the NIR region. Such an electronic absorption feature leads to a greenish solution of TbCN@C_2(5)-C_{82} in toluene (see insets of Figure 3). This spectral feature of TbCN@C_2(5)-C_{82} is obviously different from that of the reported YCN@C_s(6)-C_{82}, for which the toluene solution is brown-yellow.[9] More strikingly, the optical band gap ($\Delta E_{gap,\ optical}$) of TbCN@C_2(5)-C_{82} estimated from the absorption spectral onset of ca. 1240 nm is 1.0 eV, much larger than that of YCN@C_s(6)-C_{82} (0.77 eV).[9] It is well-known that the electronic absorptions of fullerenes are predominantly due to $\pi-\pi^*$ carbon cage transitions and depend on the isomeric structure and charge state of the carbon cage.[1,2b,17] For endohedral fullerenes, the charge state of the carbon cage is determined by the type of encapsulated species (metal(s) or metal cluster) which transfers a certain number of electrons to the carbon cage. In particular, for clusterfullerenes with the same type of metal cluster encapsulated (i.e., the charge state of the carbon cage is same), the electronic absorption property is in general dependent primarily on the isomeric structure of the carbon cage and insensitive to the encapsulated metal itself.[1,2b,17] Therefore, the difference between the electronic absorption spectra of TbCN@C_2(5)-C_{82} and YCN@C_s(6)-C_{82} is evidently resulted from their discrepancy on the cage isomeric structure.

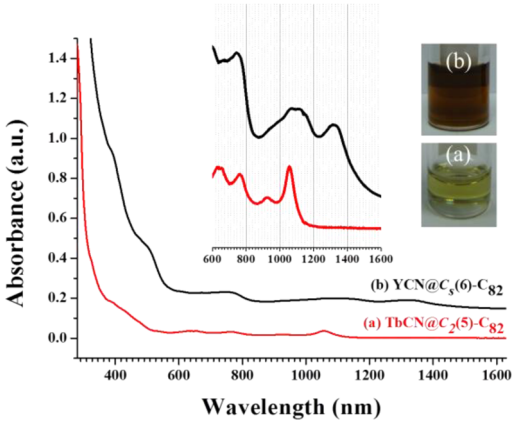

Figure 3. UV−vis−NIR spectrum of TbCN@C_2(5)-C_{82} (a) dissolved in toluene in comparison with that of YCN@C_s(6)-C_{82} (b). Spectrum of YCN@C_s(6)-C_{82} are shifted vertically for clarity. Insets: Enlarged spectral region (600−1600 nm) and the photographs of samples in toluene.

However, the UV−vis−NIR spectra of TbCN@C_2(5)-C_{82} and Yb@C_2(5)-C_{82} show a similar absorption feature but with a significant shift of the absorption peak in the region of 600−1400 nm (especially the two absorption peaks at 1056 and 923 nm). Besides, the estimated optical band gap ($\Delta E_{gap,\ optical}$) of TbCN@C_2(5)-C_{82} (1.0 eV) is also larger than that of Yb@C_2(5)-C_{82} (0.92 eV) (see Table 1).[19] These results indicate that the encapsulated species of X@C_{82} (X = TbCN, Yb) has a dramatic influence on the electronic absorption properties correlating to the molecular orbital energy level, and this conclusion is further confirmed by electrochemical study below.

The FTIR spectrum of TbCN@C_2(5)-C_{82} shows a large number of vibrational lines with relatively low signal-to-noise ratio due to its relatively low cage symmetry. In specific, the broad vibrational bands from 900 to 1600 cm^{-1} assigned to the cage tangential modes look apparently different between TbCN@C_2(5)-C_{82} and YCN@C_s(6)-C_{82},[18] and this is again resulted from their discrepancy on the cage isomeric structure (see SI Figure S7).

Electrochemical Study of TbCN@C_2(5)-C_{82}. The cyclic voltammogram of TbCN@C_2(5)-C_{82} measured in *o*-dichlorobenzene (*o*-DCB) with tetrabutylammonium hexafluorophosphate ($TBAPF_6$) as supporting electrolyte is illustrated in Figure 4, which includes also that of YCN@C_s(6)-C_{82} obtained under identical conditions for comparison. The characteristic redox potentials are summarized in Table 1. In the anodic region, TbCN@C_2(5)-C_{82} exhibits one reversible oxidation step with a half-wave potential ($E_{1/2}$) at 0.50 V, which is shifted negatively compared to that of YCN@C_s(6)-C_{82} (0.56 V).[9] However, in the cathodic region, TbCN@C_2(5)-C_{82} shows four reversible reduction steps with half-wave potential ($E_{1/2}$) at −0.88, −0.97, −1.55, −1.91 V, respectively (see SI Figure S8).

Table 1. Redox Potentials (V vs Fc/Fc^+), Electrochemical Energy Gaps ($\Delta E_{gap,\ EC}$) and Optical Band-Gaps ($\Delta E_{gap,\ optical}$) of TbCN@C_2(5)-C_{82}, YCN@C_s(6)-C_{82}, and Yb@C_2(5)-C_{82}

	$E_{1/2}$ (V vs Fc/Fc^+)								
	reduction steps (E_{red})				oxidation step (E_{ox})				
samples	first	second	third	fourth	first	$\Delta E_{gap,\ EC}$/V[a]	absorption onset (λ_{onset}, nm)	$\Delta E_{gap,\ optical}$/eV[b]	ref
TbCN@C_2(5)-C_{82}	−0.88	−0.97	−1.55	−1.91	0.50	1.38	1240	1.0	this work
Yb@C_2(5)-C_{82}	−0.86	−0.98	−1.50	−1.87	0.38	1.24	1350[c]	0.92	19
YCN@C_s(6)-C_{82}	−0.59	−0.84	−1.76	−1.92	0.56	1.15	1620	0.77	9

[a] $\Delta E_{gap,EC} = E_{1/2,ox(1)} - E_{1/2,red(1)}$. [b] $\Delta E_{gap,optical} = 1240/\lambda_{onset}$. [c] Estimated from ref 19.

dx.doi.org/10.1021/ic500353k | Inorg. Chem. 2014, 53, 5201−5205

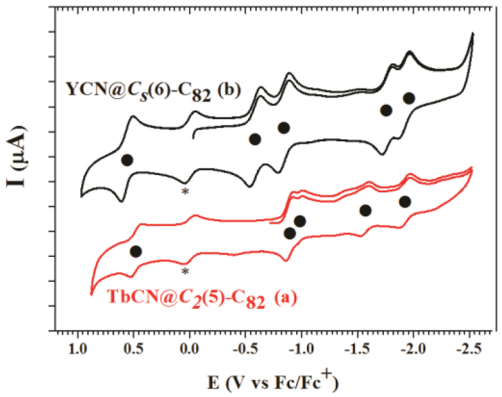

Figure 4. Cyclic voltammograms of TbCN@C_2(5)-C_{82} (a) and YCN@C_s(6)-C_{82} (b) in *o*-DCB solution. Ferrocene (Fc) was added as the internal standard, $TBAPF_6$ as supporting electrolyte, scan rate: 100 mV·s^{-1}. The half-wave potentials ($E_{1/2}$) of each redox step are marked with a solid dot to aid comparison. The asterisk labels the oxidation peak of ferrocene.

Obviously, the first and second reduction potentials of TbCN@C_2(5)-C_{82} are both shifted negatively relative to those of YCN@C_s(6)-C_{82} (see Figure 4 and Table 1). Besides, similar to the case of YCN@C_s(6)-C_{82}, which shows a large separation (0.92 V) between the second and third reduction steps, for TbCN@C_2(5)-C_{82}, the separation between the second and third reduction steps (0.58 V) is also much larger than those between the first two reduction steps (first-second, 0.09 V) and the last two reduction steps (third-fourth, 0.36 V).[9] Moreover, for TbCN@C_2(5)-C_{82}, its first two reduction steps are mutually very close with a separation of only 0.09 V, suggesting that TbCN@C_2(5)-C_{82} has a closed-shell electronic configuration with nondegenerate low-lying LUMO and accessible LUMO+1 orbitals.[19]

Interestingly, the reduction steps of TbCN@C_2(5)-C_{82} show a high resemblance to that of the reported Yb@C_2(5)-C_{82},[19] and the difference of reduction potentials between TbCN@C_2(5)-C_{82} and Yb@C_2(5)-C_{82} is less than 0.05 V (see Table 1).[19] This confirms further our assignment of the C_2(5)-C_{82} isomeric cage to TbCN@C_{82}. However, the first oxidation potential of TbCN@C_2(5)-C_{82} is positively shifted by 0.12 V compared to that of Yb@C_2(5)-C_{82}. These results indicate clearly that the encapsulated species of X@C_{82} (X=TbCN, Yb) has a dramatic influence on the oxidation property correlating to the HOMO level, whereas its influence on the reduction property, which correlates to the LUMO levels, is negligible.

On the basis of the similarity of the reduction steps of TbCN@C_2(5)-C_{82} with that of Yb@C_2(5)-C_{82}, a similar electronic configuration to that of Yb@C_2(5)-C_{82}, $[Tb^{3+}(CN)^-]^{2+}@[C_2(5)\text{-}C_{82}]^{2-}$, can be expected for TbCN@C_2(5)-C_{82}. Accordingly, the formal valence state of Tb within TbCN@C_2(5)-C_{82} is expected to be +3. Taking the electronic configuration of $[Xe]4f^8$ for Tb^{3+} into account, six unpaired electrons exist. Thus, it is intriguing to address whether TbCN@C_2(5)-C_{82} is paramagnetic or not. Our ESR measurement of TbCN@C_2(5)-C_{82} revealed no signal even at temperatures as low as 77 K. This is consistent with the proposed valency of Tb^{3+} because it is well-known that the ESR signal of Tb^{3+} ion could not be observed at $T > 30$ K due to its fast spin−lattice relaxation.[20] A similar ESR-silent behavior was reported for another Tb-based endohedral fullerene $Tb_2@C_{79}N$ in which Tb takes a +3 valence state as well.[8a]

CONCLUSIONS

In summary, we have successfully synthesized and isolated TbCN@C_2(5)-C_{82} as the first Tb-based monometallic CYCF, whose structure was determined unambiguously to be TbCN@C_2(5)-C_{82} by single crystal X-ray diffraction study, and the C−N bond length within the encaged TbCN cluster is 0.94(5) Å, which is smaller by at least 0.17 Å than those of the reported C−N triple bonds in traditional cyanide/nitrile compounds and cyano coordination complexes but nearly the same to that found for YCN@C_s(6)-C_{82}. An electronic configuration of $[Tb^{3+}(CN)^-]^{2+}@[C_2(5)\text{-}C_{82}]^{2-}$ was proposed for TbCN@C_2(5)-C_{82}. TbCN@C_2(5)-C_{82} represents the second entrant of the CYCF family, and its successful isolation paves the way for exploring novel endohedral fullerenes with CYCF as a general platform.

EXPERIMENTAL SECTION

Synthesis and Isolation of TbCN@C_2(5)-C_{82}. TbCN@C_2(5)-C_{82} was synthesized in a modified Krätschmer-Huffman fullerene generator by vaporizing composite graphite rods (Φ8 × 150 mm) containing a mixture of Tb_4O_7 and graphite powder (molar ratio of Tb:C = 1:15) with the addition of 10 mbar N_2 into 400 mbar He as previously described.[9,11] To investigate the effect of TiO_2 on the formation of TbCN@C_{82}, a reference synthesis by using a mixture of Tb_4O_7 (99.99%), TiO_2 (99.99%), and graphite powder with a molar ratio of 1:1:15 (Tb/Ti/C) was also carried out. The as-produced soot was Soxhlet-extracted by CS_2 for 24 h, and the resulting brown-yellow solution was distilled to remove CS_2 and then immediately redissolved in toluene and subsequently passed through a 0.2 μm Telflon filter (Sartorius AG, Germany) for HPLC separation. The isolation of TbCN@C_2(5)-C_{82} was performed by three-step HPLC. The purity of the isolated TbCN@C_2(5)-C_{82} was further checked by laser desorption/ionization time-of-flight (LD-TOF) mass spectroscopic (MS) analysis (Biflex III, Bruker Daltonics Inc., Germany).

Spectroscopic Characterizations. UV−vis−NIR spectra were recorded on a UV−vis−NIR 3600 spectrometer (Shimadzu, Japan) using a quartz cell of 1 mm layer thickness and 1 nm resolution with the samples dissolved in toluene. For FTIR measurement, the samples were drop-coated onto KBr single-crystal disks. The residual toluene was removed by heating the polycrystalline films in a vacuum of 2 × 10^{-6} mbar at 235 °C for 3 h. FTIR spectra were recorded at room temperature on a TENSOR 27 spectrometer (Bruker, Germany). ESR spectra were measured in toluene solution using a JES-FA200 FT-EPR X-band spectrometer (JEOL, Japan).

Electrochemical Study. Electrochemical study was performed in o-dichlorobenzene (o-DCB, anhydrous, 99%, Aldrich). The supporting electrolyte was tetrabutylammonium hexafluorophosphate ($TBAPF_6$, puriss. electrochemical grade, Fluka) which was dried under reduced pressure at 340 K for 24 h and stored in glovebox prior to use. Cyclic voltammogram experiments were performed with a CHI 660 potentiostat (CHI Instrument, U.S.A.) at room temperature in a glovebox. A standard three-electrode arrangement of a platinum (Pt) wire as working electrode, a platinum coil as counter electrode, and a silver wire as a pseudoreference electrode was used. In a comparison experiment, ferrocene (Fc) was added as the internal standard and all potentials are referred to the Fc/Fc^+ couple.

X-ray Crystallographic Study of TbCN@C_2(5)-C_{82}. Crystal growth of TbCN@C_2(5)-C_{82}·Ni^{II}(OEP)·$2C_6H_6$ was accomplished by layering a solution of 1 mg Ni^{II}(OEP) (OEP = octaethylporphyrin) in 1 mL benzene over a solution of ca. 1 mg of TbCN@C_2(5)-C_{82} in 2 mL benzene. After the two solutions diffused together over a period of one month, small black crystals suitable for X-ray crystallographic study formed upon a slow evaporation of benzene. X-ray diffraction data collection for the crystal of TbCN@C_2(5)-C_{82}·Ni^{II}(OEP)·$2C_6H_6$ (0.01 × 0.02 × 0.01 mm^3) was carried out at 100 K on an Agilent Supernova diffractometer (Agilent Technologies, U.S.A.) with a Cu radiation (λ = 1.54178 Å). TbCN@C_2(5)-C_{82}·Ni^{II}(OEP)·$2C_6H_6$

dx.doi.org/10.1021/ic500353k | Inorg. Chem. 2014, 53, 5201−5205

crystallizes in the monoclinic space group $C2/m$, a = 25.320(1) Å, b = 14.975(1) Å, c = 19.886(1) Å, β = 94.325(5)°, V = 7518.6(7) Å^3, Z = 4. A numerical absorption correction utilizing equivalents was employed. The structure was solved by direct methods and refined using all data (based on F^2) by SHELX 97.[21] Hydrogen atoms were located in a difference map, added geometrically, and refined with a riding model. Refinement of 7346 reflections, 1039 parameters, and 6656 restraints yielded wR_2 = 0.3119 for all data and a conventional $R1$ of 0.1020 based on 4725 reflections with $I > 2\sigma(I)$.

■ ASSOCIATED CONTENT

Supporting Information

Isolation of TbCN@C_2(5)-C_{82}, X-ray crystallographic data of TbCN@C_2(5)-C_{82}, FTIR spectra of TbCN@C_2(5)-C_{82} and YCN@C_s(6)-C_{82}, cyclic voltammograms of TbCN@C_2(5)-C_{82} in different scanning regions, and X-ray crystallographic file in CIF format for TbCN@C_2(5)-C_{82}·Ni^{II}(OEP)·2C_6H_6 and so forth. This material is available free of charge via the Internet at http://pubs.acs.org.

■ AUTHOR INFORMATION

Corresponding Author

*E-mail: sfyang@ustc.edu.cn.

Notes

The authors declare no competing financial interest.

■ ACKNOWLEDGMENTS

This work is partially supported by the National Natural Science Foundation of China (Nos. 21132007, 21371164) and National Basic Research Program of China (2010CB923300, 2011CB921400).

■ REFERENCES

(1) For recent reviews, see (a) Popov, A. A.; Yang, S. F.; Dunsch, L. *Chem. Rev.* **2013**, *113*, 5989. (b) Wang, T. S.; Wang, C. R. *Acc. Chem. Res.* **2014**, *47*, 450. (c) Lu, X.; Feng, L.; Akasaka, T.; Nagase, S. *Chem. Soc. Rev.* **2012**, *41*, 7723. (d) Yang, S. F. *Curr. Org. Chem.* **2012**, *16*, 1079. (e) Rodriguez-Fortea, A.; Balch, A. L.; Poblet, J. M. *Chem. Soc. Rev.* **2011**, *40*, 3551. (f) Yang, S. F.; Liu, F. P.; Chen, C. B.; Jiao, M. Z.; Wei, T. *Chem. Commun.* **2011**, *47*, 11822. (g) Chaur, M. N.; Melin, F.; Ortiz, A. L.; Echegoyen, L. *Angew. Chem., Int. Ed.* **2009**, *48*, 7514.

(2) (a) Stevenson, S.; Rice, G.; Glass, T.; Harich, K.; Cromer, F.; Jordan, M. R.; Craft, J.; Hadju, E.; Bible, R.; Olmstead, M. M.; Maitra, K.; Fisher, A. J.; Balch, A. L.; Dorn, H. C. *Nature* **1999**, *401*, 55. (b) Zhang, J. Y.; Stevenson, S.; Dorn, H. C. *Acc. Chem. Res.* **2013**, *46*, 1548.

(3) (a) Wang, C. R.; Kai, T.; Tomiyama, T.; Yoshida, T.; Kobayashi, Y.; Nishibori, E.; Takata, M.; Sakata, M.; Shinohara, H. *Angew. Chem., Int. Ed.* **2001**, *40*, 397. (b) Lu, X.; Akasaka, T.; Nagase, S. *Acc. Chem. Res.* **2013**, *46*, 1627.

(4) Stevenson, S.; Mackey, M. A.; Stuart, M. A.; Phillips, J. P.; Easterling, M. L.; Chancellor, C. J.; Olmstead, M. M.; Balch, A. L. *J. Am. Chem. Soc.* **2008**, *130*, 11844.

(5) Dunsch, L.; Yang, S. F.; Zhang, L.; Svitova, A.; Oswald, S.; Popov, A. A. *J. Am. Chem. Soc.* **2010**, *132*, 5413.

(6) Krause, M.; Ziegs, F.; Popov, A. A.; Dunsch, L. *ChemPhysChem* **2007**, *8*, 537.

(7) Wang, T. S.; Feng, L.; Wu, J. Y.; Xu, W.; Xiang, J. F.; Tan, K.; Ma, Y. H.; Zheng, J. P.; Jiang, L.; Lu, X.; Shu, C. Y.; Wang, C. R. *J. Am. Chem. Soc.* **2010**, *132*, 16362.

(8) (a) Zuo, T.; Xu, L.; Beavers, C. M.; Olmstead, M. M.; Fu, W.; Crawford, T. D.; Balch, A. L.; Dorn, H. C. *J. Am. Chem. Soc.* **2008**, *130*, 12992. (b) Fu, W.; Zhang, J.; Fuhrer, T.; Champion, H.; Furukawa, K.; Kato, T.; Mahaney, J. E.; Burke, B. G.; Williams, K. A.; Walker, K.; Dixon, C.; Ge, J. C.; Shu, C. Y.; Harich, K.; Dorn, H. C. *J. Am. Chem. Soc.* **2011**, *133*, 9741.

(9) Yang, S. F.; Chen, C. B.; Liu, F. P.; Xie, Y. P.; Li, F. Y.; Jiao, M. Z.; Suzuki, M.; Wei, T.; Wang, S.; Chen, Z. F.; Lu, X.; Akasaka, T. *Sci. Rep.* **2013**, *3*, 1487.

(10) (a) Stevenson, S.; Chancellor, C. J.; Lee, H. M.; Olmstead, M. M.; Balch, A. L. *Inorg. Chem.* **2008**, *47*, 1420. (b) Zuo, T.; Beavers, C. M.; Duchamp, J. C.; Campbell, A.; Dorn, H. C.; Olmstead, M. M.; Balch, A. L. *J. Am. Chem. Soc.* **2007**, *129*, 2035. (c) Beavers, C. M.; Zuo, T. M.; Duchamp, J. C.; Harich, K.; Dorn, H. C.; Olmstead, M. M.; Balch, A. L. *J. Am. Chem. Soc.* **2006**, *128*, 11352. (d) Feng, L.; Xu, J. X.; Shi, Z. J.; He, X. R.; Gu, Z. N. *Chem. J. Chin. Univ. Chin.* **2002**, *23*, 996.

(11) (a) Yang, S. F.; Chen, C. B.; Popov, A. A.; Zhang, W. F.; Liu, F. P.; Dunsch, L. *Chem. Commun.* **2009**, 6391. (b) Chen, C. B.; Liu, F. P.; Li, S. J.; Wang, N.; Popov, A. A.; Jiao, M. Z.; Wei, T.; Li, Q. X.; Dunsch, L.; Yang, S. F. *Inorg. Chem.* **2012**, *51*, 3039. (c) Liu, F. P.; Wei, T.; Wang, S.; Guan, J.; Lu, X.; Yang, S. F. *Fuller. Nanotub. Carbon Nanostruct.* **2014**, *22*, 215.

(12) (a) Olmstead, M. M.; Costa, D. A.; Maitra, K.; Noll, B. C.; Phillips, S. L.; Van Calcar, P. M.; Balch, A. L. *J. Am. Chem. Soc.* **1999**, *121*, 7090. (b) Yang, H.; Yu, M.; Jin, H.; Liu, Z.; Yao, M.; Liu, B.; Olmstead, M. M.; Balch, A. L. *J. Am. Chem. Soc.* **2012**, *134*, 5331. (c) Yang, H.; Jin, H.; Wang, X.; Liu, Z.; Yu, M.; Zhao, F.; Mercado, B. Q.; Olmstead, M. M.; Balch, A. L. *J. Am. Chem. Soc.* **2012**, *134*, 14127. (d) Suzuki, M.; Slanina, Z.; Mizorogi, N.; Lu, X.; Nagase, S.; Olmstead, M. M.; Balch, A. L.; Akasaka, T. *J. Am. Chem. Soc.* **2012**, *134*, 18772. (e) Yang, H.; Jin, H.; Zhen, H.; Wang, Z.; Liu, Z.; Beavers, C. M.; Mercado, B. Q.; Olmstead, M. M.; Balch, A. L. *J. Am. Chem. Soc.* **2011**, *133*, 6299. (f) Lu, X.; Lian, Y.; Beavers, C. M.; Mizorogi, N.; Slanina, Z.; Nagase, S.; Akasaka, T. *J. Am. Chem. Soc.* **2011**, *133*, 10772. (g) Yang, H.; Jin, H.; Hong, B.; Liu, Z.; Beavers, C. M.; Zhen, H.; Wang, Z.; Mercado, B. Q.; Olmstead, M. M.; Balch, A. L. *J. Am. Chem. Soc.* **2011**, *133*, 16911. (h) Beavers, C. M.; Jin, H.; Yang, H.; Wang, Z.; Wang, X.; Ge, H.; Liu, Z.; Mercado, B. Q.; Olmstead, M. M.; Balch, A. L. *J. Am. Chem. Soc.* **2011**, *133*, 15338. (i) Xu, W.; Feng, L.; Calvaresi, M.; Liu, J.; Liu, Y.; Niu, B.; Shi, Z.; Lian, Y.; Zerbetto, F. *J. Am. Chem. Soc.* **2013**, *135*, 4187.

(13) Xu, W.; Niu, B.; Feng, L.; Shi, Z. J.; Lian, Y. F. *Chem.—Eur. J.* **2012**, *18*, 14246.

(14) (a) Kurihara, H.; Lu, X.; Iiduka, Y.; Nikawa, H.; Hachiya, M.; Mizorogi, N.; Slanina, Z.; Tsuchiya, T.; Nagase, S.; Akasaka, T. *Inorg. Chem.* **2012**, *51*, 746. (b) Mercado, B. Q.; Olmstead, M. M.; Beavers, C. M.; Easterling, M. L.; Stevenson, S.; Mackey, M. A.; Coumbe, C. E.; Phillips, J. D.; Phillips, J. P.; Poblet, J. M.; Balch, A. L. *Chem. Commun.* **2010**, *46*, 279.

(15) (a) Harris, K. J.; Wasylishen, R. E. *Inorg. Chem.* **2009**, *48*, 2316. (b) Stevens, P. A.; Madix, R. J.; Stohr, J. *J. Chem. Phys.* **1989**, *91*, 4338. (c) Orpen, A. G.; Brammer, L.; Allen, F. H.; Kennard, O.; Watson, D. G.; Taylor, R. *J. Chem. Soc., Dalton Trans.* **1989**, S1.

(16) Yang, H.; Lu, C. X.; Liu, Z. Y.; Jin, H. X.; Che, Y. L.; Olmstead, M. M.; Balch, A. L. *J. Am. Chem. Soc.* **2008**, *130*, 17296.

(17) (a) Dunsch, L.; Yang, S. *Small* **2007**, *3*, 1298. (b) Dunsch, L.; Yang, S. *Phys. Chem. Chem. Phys.* **2007**, *9*, 3067.

(18) Krause, M.; Kuzmany, H.; Georgi, P.; Dunsch, L.; Vietze, K.; Seifert, G. *J. Chem. Phys.* **2001**, *115*, 6596.

(19) Lu, X.; Slanina, Z.; Akasaka, T.; Tsuchiya, T.; Mizorogi, N.; Nagase, S. *J. Am. Chem. Soc.* **2010**, *132*, 5896.

(20) (a) Altshuler, S. A.; Kozyrev, B. M. *Electron Paramagnetic Resonance in Compounds of Transition Elements*, 2nd ed.; John Wiley & Sons: New York, 1974. (b) Gafurov, M. R.; Ivanshin, V. A.; Kurkin, I. N.; Rodionova, M. P.; Keller, H.; Gutmann, M.; Staub, U. *J. Magn. Reson.* **2003**, *161*, 210.

(21) Sheldrick, G. *Acta Crystallogr. A* **2008**, *64*, 112.

dx.doi.org/10.1021/ic500353k | *Inorg. Chem.* 2014, 53, 5201−5205